VIP Nanocatalysis Very Important Paper

Deutsche Ausgabe: DOI: 10.1002/ange.201510643
Internationale Ausgabe: DOI: 10.1002/anie.201510643

Catalytically Active Rh Sub-Nanoclusters on TiO_2 for CO Oxidation at Cryogenic Temperatures

Hongling Guan[+], Jian Lin[+], Botao Qiao, Xiaofeng Yang, Lin Li, Shu Miao, Jingyue Liu, Aiqin Wang, Xiaodong Wang, and Tao Zhang**

Abstract: *The discovery that gold catalysts could be active for CO oxidation at cryogenic temperatures has ignited much excitement in nanocatalysis. Whether the alternative Pt group metal (PGM) catalysts can exhibit such high performance is an interesting research issue. So far, no PGM catalyst shows activity for CO oxidation at cryogenic temperatures. In this work, we report a sub-nano Rh/TiO_2 catalyst that can completely convert CO at 223 K. This catalyst exhibits at least three orders of magnitude higher turnover frequency (TOF) than the best Rh-based catalysts and comparable to the well-known Au/TiO_2 for CO oxidation. The specific size range of 0.4–0.8 nm Rh clusters is critical to the facile activation of O_2 over the Rh–TiO_2 interface in a form of Rh−O−O−Ti (superoxide). This superoxide is ready to react with the CO adsorbed on TiO_2 sites at cryogenic temperatures.*

Low-temperature CO oxidation is not only valuable as a typical probe reaction for fundamental studies but also important for practical applications. Pt group metal (PGM) catalysts are widely used to catalyze CO oxidation in automotive emission control and purification of gas streams derived from petrochemical industry.[1] Since Langmuir's pioneering work, CO oxidation on PGM has been studied for almost a century, and found to generally follow a Langmuir–Hinshelwood (L–H) mechanism.[2] The key issue is that the strongly adsorbed CO on PGM significantly inhibits the adsorption and activation of O_2; high working temperatures (e.g. higher than 373 K) are thus required to weaken the strength of CO adsorption and make the adsorbed O_2 facile.[3] Various strategies, such as downsizing PGM particles from nano to single atoms,[4] and engineering the metal–metal oxide (hydroxide) interfaces,[5] have been proposed either to weaken CO adsorption on PGM sites or to promote O_2 adsorption on alternative sites. Although these strategies significantly improved the activity of PGM catalysts, it has been a grand challenge to use PGM catalysts for CO oxidation at ambient temperatures, not to mention cryogenic temperatures.

One classical catalyst for CO oxidation at cryogenic temperatures is oxide supported Au nanoparticles first discovered by Haruta et al.[6] The learnings and insights gained from studies of supported Au catalysts have provided guidance to design and develop PGM catalysts with much improved performance.[7] There seems to be, however, a barrier for CO oxidation on PGM catalysts at cryogenic temperatures. The difficulties lie in the much higher adsorption strength of CO on PGM than on Au;[8] furthermore, the activation of O_2 is generally regarded as a key step in CO oxidation. However, O_2 is easily dissociated to atomic oxygen species on PGM[9] which can only react with CO above room temperature.[10] Thus, a fundamental question still remains, that is, whether PGM can ever be active at cryogenic temperatures.

Recently, Yates and co-workers discovered a new reaction mechanism for CO oxidation on Au/TiO_2 that the rather weaker adsorption of CO on TiO_2 sites diffused to react with the O_2 activated at the interface between Au and TiO_2, thus realizing CO oxidation at cryogenic temperatures.[11] We wonder if such mechanism can be feasible on PGM catalysts and make them catalytically active at cryogenic temperatures. Herein, we report a novel Rh/TiO_2 catalyst with the Rh species highly dispersed in a sub-nano scale of 0.4–0.8 nm. It is proposed that O_2 is facilely activated as Rh−O−O−Ti (superoxide) at the Rh−Ti perimeter sites when the Rh is present as sub-nano species. The superoxide reacts with the weakly adsorbed CO on the TiO_2 sites, resulting in an unexpectedly high activity with total CO conversion at 223 K. Moreover, the turnover frequency (TOF) on these sub-nanoclusters is around five times higher than that on single or pseudo single atoms and one order of magnitude higher than that on nanoparticles. This unique Rh/TiO_2 catalyst proves to be the most active Rh catalyst and its performance rivals the standard Au/TiO_2 catalyst from World Gold Council (Au/TiO_2-WGC).

The Rh/TiO_2 catalyst was synthesized by deposition-precipitation of $RhCl_3$ onto commercial TiO_2 (Degussa-P25) with a Rh loading of 2.5 wt%. Some basic physicochemical properties of the catalyst are listed in Table S1 in the Supporting Information. The XRD patterns (Figure S1) suggest a well-defined P25 crystal and there are no structural changes after the loading of Rh. The absence of any Rh-

[*] H. Guan,[+] Dr. J. Lin,[+] Dr. B. Qiao, Dr. X. Yang, Dr. L. Li, Dr. S. Miao, Prof. A. Wang, Prof. X. Wang, Prof. T. Zhang
State Key Laboratory of Catalysis
Dalian Institute of Chemical Physics
Chinese Academy of Sciences
Dalian 116023 (China)
E-mail: xdwang@dicp.ac.cn
taozhang@dicp.ac.cn
H. Guan[+]
University of Chinese Academy of Sciences
Beijing 100049 (China)
Prof. J. Liu
Department of Physics, Arizona State University
Tempe, AZ, 85287 (USA)
[+] These authors contributed equally to this work.

Supporting information for this article is available on the WWW under http://dx.doi.org/10.1002/anie.201510643.

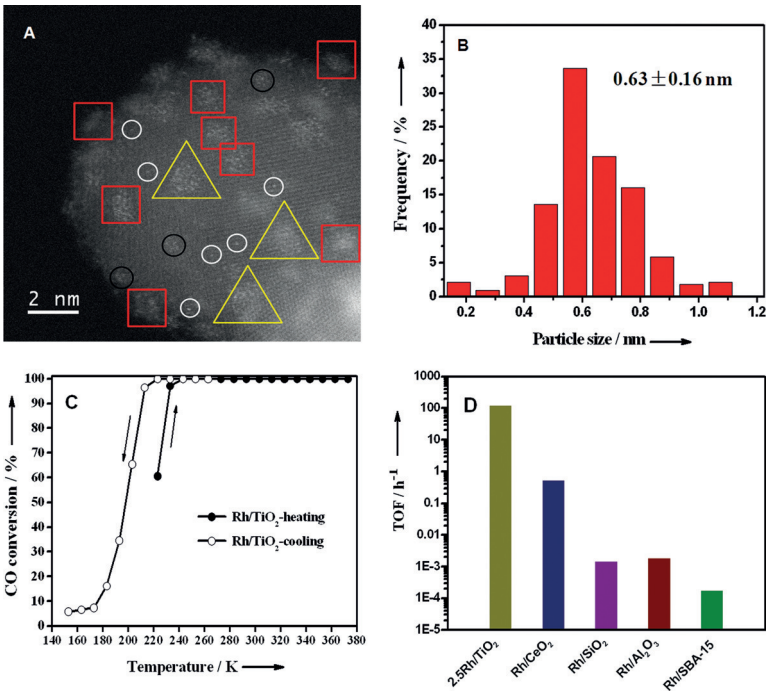

Figure 1. A) Typical HAADF-STEM images of 2.5 Rh/TiO_2. The Rh species are highly dispersed as single atom (white circles) or pseudo single atoms (black circles), sizes at 0.4–0.8 nm (red square), Rh sizes larger than 0.8 nm (yellow triangle). B) Histogram of size distributions. The size distributions were obtained by analyzing 200–400 Rh species from HAADF-STEM images. C) CO conversions as a function of reaction temperature upon heating and cooling at a rate of 2 K min^{-1} over Rh/TiO_2 catalyst. Reaction conditions: 1 vol% CO, 5 vol% O_2, and balance He. Weight hourly space velocity (WHSV): 720 000 mL g_{Rh}^{-1} h^{-1}. D) Histogram of TOF values at 293 K on Rh/TiO_2 compared with other representative Rh-based catalysts.

containing crystal phases confirms the high dispersion of the Rh species. The typical high-angle annular dark-filed scanning transmission electron microscopy (HAADF-STEM) images are presented in Figure 1 A,B and Figure S2. By detailed analyses of these images we conclude that the Rh species are highly dispersed as sub-nanoclusters with sizes ranging from 0.4 to 0.8 nm. The XPS data in Table S1 and Figure S3 show the binding energy of 307.1 and 308.2 eV, indicating the presence of both Rh^0 and RhO_x $(0<x<1)$ species in the reduced catalyst.[12]

Figure 1 C illustrates the profiles of CO conversions as a function of reaction temperatures upon heating and cooling. The CO conversion over Rh/TiO_2 catalyst is as high as 97% at 233 K and reaches 100% at 243 K. Upon cooling, it exhibits a light-off (10% conversion) temperature of 173 K and 100% conversion at 223 K. Conventionally, the PGM catalysts have poor activity for CO oxidation at such low temperatures. While the temperature for total CO conversion on this Rh/TiO_2 catalyst is even at least 100 K lower than the most active Rh-based catalyst.[13] A hysteresis is observed between the cooling and heating process, which can be explained by the changes in Rh oxidation state or by the different CO or O_2 coverage in these two processes.[14]

To further quantify the activity of the Rh/TiO_2 catalyst we measured the specific rate and turnover frequency (TOF) under a differential condition and compared these values with those of the best catalysts reported in literatures. As a benchmark, the Au/TiO_2-WGC was firstly tested. As shown in Table S2, both the specific rate (0.024 mol_{co} g_{Rh}^{-1} h^{-1}) and the TOF (7.9 h^{-1}) over Rh/TiO_2 at 193 K are comparable with those over Au/TiO_2-WGC (0.021 mol_{co} g_{Au}^{-1} h^{-1} and 15.2 h^{-1}, respectively), demonstrating the extremely high activity of the Rh/TiO_2 at cryogenic temperatures. There are no reports that Rh-based catalysts can be active at temperatures below 273 K. To compare with the published data on Rh-based catalysts, we measured the specific rate and TOF of our Rh/TiO_2 catalyst at room temperature. As shown in Figure S4, the TOF profiles in terms of CO conversion and CO_2 production are closely resembled with a rather constant value of around 120 h^{-1}. Therefore, a TON of 120 could be obtained only in the first hour which is far higher than 1. These results indicate a true catalytic process of oxidation of CO to CO_2 over Rh/TiO_2 catalyst rather than a non-catalytic consumption. Moreover, as shown in Figure 1 D and Table S2, our Rh/TiO_2 catalyst exhibits 3 orders of magnitude higher TOF than the most active Rh-based catalyst. The apparent activation energy was determined to be 13.6 kJ mol^{-1} for CO oxidation on Rh/TiO_2 (Figure S5), which is similar to that on Au/TiO_2 (14.8 kJ mol^{-1}) and much lower than that on other Rh-based catalysts. The experimentally observed outstanding performance correlates well with its lower activation barrier for CO oxidation.

The particle size is critical for CO oxidation on Au-based catalysts.[15] For Rh/TiO_2, we quantified the size distribution of Rh species from single or pseudo single atoms, sub-nano- to nanoscale with the aberration-corrected HAADF-STEM technique. The corresponding results are displayed in Figure 1, Figures S6–S9, and Table S3. The TOF values versus the Rh sizes are shown in Figure 2. The data unambiguously demonstrate that the TOF of the 0.4–0.8 nm Rh clusters is about five times higher than that of the single or

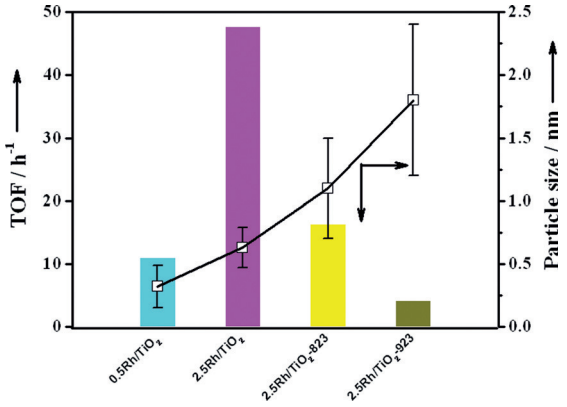

Figure 2. TOF values at 233 K and the mean size of Rh species on different Rh/TiO_2 catalysts. The size distributions of various catalysts were presented in Figure 1 and Figures S6–S8.

pseudo single atoms and one order of magnitude higher than that on nanoparticles around 1.8 nm in diameter. These detailed analyses indicate that a unique configuration of sub-nano Rh clusters is best for CO oxidation at cryogenic temperatures.

The above results show that TiO_2 supported sub-nano Rh clusters exhibit an unprecedentedly high activity for CO oxidation, even at cryogenic temperatures. In situ DRIFT measurements were performed to investigate the nature of the adsorbed CO species ($CO_{(ad)}$). As shown in Figure S10a and Table S4, four peaks on fresh Rh/TiO_2 are attributed to bridged-CO (1863 cm^{-1}), linear-CO on Rh^0 (2073 cm^{-1}), and the symmetric and asymmetric vibration of gem-dicarbonyl doublet-CO on positively charged Rh atoms (2102 and 2033 cm^{-1}), respectively. In addition, a feature at 2179 cm^{-1} is observed and can be assigned to $CO_{(ad)}$ on TiO_2.[11] The pre-adsorption of O_2 on Rh/TiO_2 leads to a significant decrease of the linear- and bridged-CO but the main presence of gem-dicarbonyl (Figure S10b), suggesting that the Rh species are easily oxidized after O_2 adsorption. It also corroborates the XPS results that a facile cycle of redox Rh species exists and that the binding energies increase after CO oxidation and then recover after reduction treatment (Figure S3). Moreover, the presence of the band at 2345 cm^{-1} suggests that even at 123 K the CO_2 formation occurs as soon as the CO is in contact with the pre-adsorbed O_2. The evolution of $CO_{(ad)}$ and CO_2 formation with time is shown in Figure 3 A. The $CO_{(ad)}$ on TiO_2 increase along with the CO_2 peak while those on Rh keep unchanged. To confirm the active adsorbed CO species, we reversed the order of adsorption. As shown in Figure 3 B, after introducing O_2 to the catalyst pre-adsorbed with CO, the $CO_{(ad)}$ on Rh still keep unchanged while the $CO_{(ad)}$ on TiO_2 decrease gradually with the increase of CO_2 peak. Figure 3 C presents the evolution of the integrated areas of CO_2, $CO_{(ad)}$ on TiO_2 and $CO_{(ad)}$ on Rh. These results unequivocally demonstrate that the active species are $CO_{(ad)}$ on TiO_2 instead of on Rh at cryogenic temperatures. This is similar to a recent finding that on Au/TiO_2 catalyst the active species in CO oxidation are CO adsorbed on TiO_2.[11] Without the presence of Rh, exposing O_2 to pure TiO_2 with pre-adsorbed $CO_{(ad)}$ does not produce any CO_2 (Figure S11). This result suggests that the adsorption of CO on TiO_2 is necessary but not sufficient for the high activity of Rh/TiO_2 at cryogenic temperatures.

Another important factor for CO oxidation is related to the active species of O_2. Electron paramagnetic resonance (EPR) is a well-accepted approach to study the O_2 adsorption and subsequent reaction.[16] As shown in Figure 4 A, the fresh Rh/TiO_2 catalyst shows a symmetric signal at $g = 2.002$, which is due to unpaired electrons trapped at the oxygen vacancies on TiO_2.[17] As shown in the TPR results (Figure S12), an obvious sharp peak exists at 259 K with H_2 consumption of 685 μmol g_{cat}^{-1} which is higher than the theoretical amount of reducing Rh^{3+} to Rh^0 (364 μmol g_{cat}^{-1}). This indicates that the TiO_2 surface in close proximity with the Rh clusters may have been reduced, resulting in the formation of oxygen vacancies. After the adsorption of O_2, the intensity of the peak at $g =$ 2.002 decreases, indicating the occupancy of oxygen vacancies by the adsorbed oxygen. Three new peaks at $g_{xx} = 2.001$, $g_{yy} =$ 2.010, $g_{zz} = 2.030$, characteristic of molecular superoxide (O_2^-) species,[17] appear. Exposure of this sample to CO results in the disappearance of these peaks and the reoccurrence of the peak at $g = 2.002$, a consequence of the recovery of oxygen vacancies through the reaction between O_2^- and CO.

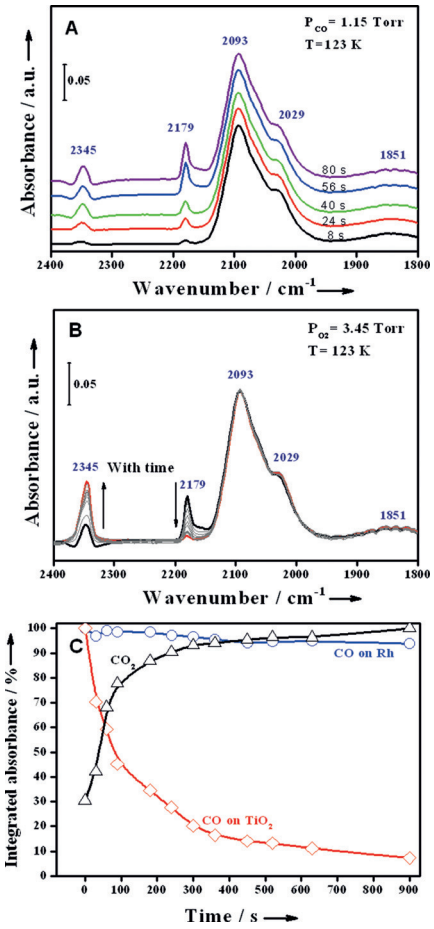

Figure 3. A) Evolution of infrared spectra at 123 K after introducing CO to the O_2 pre-adsorbed Rh/TiO_2 sample. B) Evolution of infrared spectra at 123 K after introducing O_2 to the CO pre-adsorbed Rh/TiO_2 sample. C) Plots of relative integrated absorbance of CO adsorbed on Rh or TiO_2 and CO_2 with time derived from results of Figure 3 B.

The activation of molecular superoxide through Rh-Ti-O-O, Rh-O_2-Ti or Rh–O–O–Ti was examined by DFT calculations. The Rh_5 cluster was selected according to HAADF-STEM result and was anchored on the anatase-TiO_2 (101) surface considering that there is more anatase surfaces than those of the rutile in the polymorph of P25 (Figure S13). As shown in Figure 4 B, the adsorption energy for the Rh–O–O–Ti configuration is 0.92 eV, higher than that of the other two configurations. This result suggests that the O_2 is most strongly bound to the Ti sites near the Rh species at the Rh-TiO_2 perimeters, which can lead to a relatively large order of 0.55 for O_2 (Figure S14). We further clarified the critical role of sub-nano Rh species on the activation of O_2. According to the EPR results, there is no presence of O_2^- species on the Rh/TiO_2 sample with the Rh particle sizes around 1.8 nm (Figure S15). A decreased activity for CO

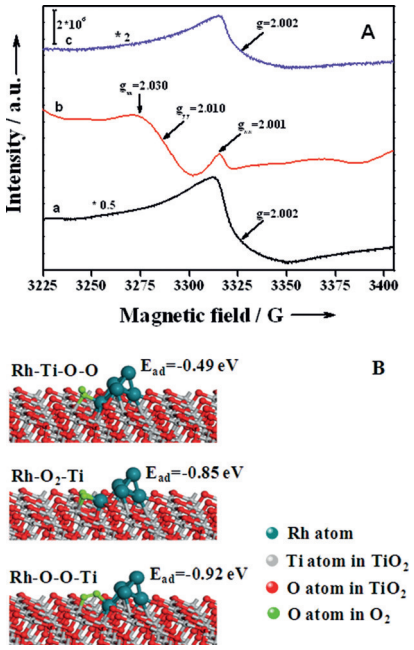

Figure 4. A) EPR spectra obtained at 100 K on the Rh/TiO_2 catalysts with different treatments. a: the fresh reduced sample; b: the sample a exposed to O_2 and then evacuated at room temperature; c: the sample b exposed to CO at room temperature. B) Different types of molecular O_2 activated on Rh/TiO_2 by DFT calculations.

oxidation is observed on such catalyst (Figure S16). In addition, the CO adsorption energy is only 0.38 eV on TiO_2 sites, much weaker than that on Rh sites as shown in Figure S17. Such weak adsorption of CO molecules renders them labile and can easily diffuse to the perimeter sites to react with the superoxide. This type of CO species does not compete with the adsorption of O_2, thus leading to a slightly positive order of CO even at cryogenic temperatures (Figure S14), in contrast to the usually negative order of CO during CO oxidation.[18] It also promotes more rapid consumption of CO(ad) on TiO_2 sites than that on Rh sites, which makes them the main species to produce CO_2, as revealed by diffuse reflectance infrared Fourier transform spectroscopy (DRIFTS) results in Figure 3B. As a result, CO oxidation could occur at cryogenic temperatures as long as CO adsorption on TiO_2 and the formation of superoxide in a form of Rh–O–O–Ti simultaneously occurs at the perimeters between sub-nano Rh and TiO_2. The stronger bonded CO species on Rh sites are kinetically inactive for CO oxidation because these species cannot desorb at such low temperatures (Figure 3C). At higher temperatures, these CO molecules can become more mobile and then participate in production of CO_2 according to traditional L–H mechanism.[2b,11]

In conclusion, we have developed a sub-nano Rh/TiO_2 catalyst with Rh species highly dispersed in a scale of 0.4–0.8 nm. This catalyst exhibits an unprecedentedly high activity of complete CO conversion at 223 K, at least 100 K lower than the ever reported Rh-based catalyst so far and at least three orders of magnitude higher TOF, even comparable with the standard Au/TiO_2 catalyst which is well-known for CO oxidation at cryogenic temperatures. Moreover, the TOF on these sub-nanoclusters is around five times higher than that on single or pseudo single atoms and one order of magnitude higher than that on nanoparticles. The superior performance of this catalyst can be attributed to the facile activation of O_2 as Rh–O–O–Ti species on the perimeters between Rh sub-nanoclusters and TiO_2 support and ready reaction with the adsorbed CO species on TiO_2 sites. The unconventional but reasonable discovery in this paper that the Rh/TiO_2 catalyst is highly active for CO oxidation at cryogenic temperatures may make people re-recognize the CO oxidation on PGM metal catalysts. It also provides an opportunity to fabricate highly active PGM catalysts by detailed understanding of the active sites.

Experimental Section

All catalysts were prepared by deposition–precipitation methods. Typically, 1 g of TiO_2-P25 was dispersed into 100 mL of deionized water and the suspension was stirred at 353 K for 15 min. Then, 100 mL of aqueous $RhCl_3 \cdot 3H_2O$ solution with appropriate concentration was added dropwise (3 mL min^{-1}) to the suspension, during which the pH value was maintained at 8.5 with NaOH solution. After stirring for 3 h and aging for 1 h, the resulting precipitate was filtered and washed with 1 L hot deionized water, then dried at 353 K overnight and calcined at 673 K for 4 h. The resulted catalysts were denoted as 2.5 Rh/TiO_2 and 0.5 Rh/TiO_2 with Rh loading of 2.5 and 0.5 wt%, respectively. For comparison, 2.5 Rh/TiO_2 was further calcined at 823 and 923 K, denoted as 2.5 Rh/TiO_2-823 and 2.5 Rh/TiO_2-923, respectively.

The details about activity tests, the characterizations such as HAADF-STEM, EPR, and DRIFTS are given in the Supplementary Information.

Acknowledgements

This work was supported by National Nature Science Foundation of China (grant numbers 21076211, 21103173, 21203181, 21303183, 21576251). J.L. is supported by the startup fund of the College of Liberal Arts and Sciences of Arizona State University. The electron microscopy data was obtained at the John M Cowley Center for High Resolution Electron Microscopy at Arizona State University. The calculations were performed at Shanghai Supercomputing Center.

Keywords: carbon monoxide oxidation · catalysis · clusters · cryogenic temperatures · rhodium

How to cite: *Angew. Chem. Int. Ed.* **2016**, *55*, 2820–2824
Angew. Chem. **2016**, *128*, 2870–2874

[1] H. Freund, G. Meijer, M. Scheffler, R. Schlögl, M. Wolf, *Angew. Chem. Int. Ed.* **2011**, *50*, 10064–10094; *Angew. Chem.* **2011**, *123*, 10242–10275.
[2] a) I. Langmuir, *Trans. Faraday Soc.* **1922**, *17*, 621–654; b) M. A. Newton, D. Ferri, G. Smolentsev, V. Marchionni, M. Nachtegaal, *Nat. Commun.* **2015**, *6*, 8675.
[3] a) K. Liu, A. Wang, T. Zhang, *ACS Catal.* **2012**, *2*, 1165–1178; b) A. D. Allian, K. Takanabe, K. Fujdala, X. Hao, T. Truex, J.

Cai, C. Buda, M. Neurock, E. Iglesia, *J. Am. Chem. Soc.* **2011**, *133*, 4498 – 4517.
[4] a) B. Qiao, A. Wang, X. Yang, L. Allard, Z. Jiang, Y. Cui, J. Liu, J. Li, T. Zhang, *Nat. Chem.* **2011**, *3*, 634 – 641; b) J. Lin, B. Qiao, J. Liu, Y. Huang, A. Wang, L. Li, W. Zhang, L. Allard, X. Wang, T. Zhang, *Angew. Chem. Int. Ed.* **2012**, *51*, 2920 – 2924; *Angew. Chem.* **2012**, *124*, 2974 – 2978; c) M. Moses-DeBusk, M. Yoon, L. F. Allard, D. R. Mullins, Z. L. Wu, X. F. Yang, G. Veith, G. M. Stocks, C. K. Narula, *J. Am. Chem. Soc.* **2013**, *135*, 12634 – 12645; d) E. J. Peterson, A. T. DeLaRiva, S. Lin, R. S. Johnson, H. Guo, J. T. Miller, J. Hun Kwak, C. H. Peden, B. Kiefer, L. F. Allard, F. H. Ribeiro, A. K. Datye, *Nat. Commun.* **2014**, *5*, 4885.
[5] a) Q. Fu, W. Li, Y. Yao, H. Liu, H. Su, D. Ma, X. Gu, L. Chen, Z. Wang, H. Zhang, B. Wang, X. Bao, *Science* **2010**, *328*, 1141 – 1144; b) M. Cargnello, V. Doan-Nguyen, T. Gordon, R. Diaz, E. Stach, R. Gorte, P. Fornasiero, C. Murray, *Science* **2013**, *341*, 771 – 773; c) G. Chen, Y. Zhao, G. Fu, P. Duchesne, L. Gu, Y. Zheng, X. Weng, M. Chen, P. Zhang, C. Pao, J. Lee, N. Zheng, *Science* **2014**, *344*, 495 – 499.
[6] M. Haruta, S. Tsubota, T. Kobayashi, H. Kageyama, M. J. Genet, B. Delmon, *J. Catal.* **1993**, *144*, 175 – 192.
[7] a) B. Qiao, L. Liu, J. Zhang, Y. Q. Deng, *J. Catal.* **2009**, *261*, 241 – 244; b) S. Golunski, *Platinum Met. Rev.* **2013**, *57*, 82 – 84; c) K. Zhao, H. Tang, B. Qiao, L. Li, J. Wang, *Acs Catal.* **2015**, *5*, 3528 – 3539.
[8] F. Abild-Pedersen, M. Andersson, *Surf. Sci.* **2007**, *601*, 1747 – 1753.
[9] T. Janssens, B. Clausen, B. Hvolbaek, H. Falsig, C. Christensen, T. Bligaard, J. Norskov, *Top. Catal.* **2007**, *44*, 15 – 26.
[10] D. Widmann, R. J. Behm, *Acc. Chem. Res.* **2014**, *47*, 740 – 749.
[11] I. Green, W. Tang, M. Neurock, J. Yates, *Science* **2011**, *333*, 736 – 739.
[12] M. Grass, Y. Zhang, D. Butcher, J. Park, Y. Li, H. Bluhm, K. Bratlie, T. Zhang, G. Somorjai, *Angew. Chem. Int. Ed.* **2008**, *47*, 8893 – 8896; *Angew. Chem.* **2008**, *120*, 9025 – 9028.
[13] D. Ligthart, R. van Santen, E. Hensen, *Angew. Chem. Int. Ed.* **2011**, *50*, 5306 – 5310; *Angew. Chem.* **2011**, *123*, 5418 – 5422.
[14] M. Lepage, T. Visser, F. Soulimani, A. M. Beale, A. Iglesias-Juez, A. M. J. van der Eerden, B. M. Weckhuysen, *J. Phys. Chem. C* **2008**, *112*, 9394 – 9404.
[15] a) M. Valden, X. Lai, D. W. Goodman, *Science* **1998**, *281*, 1647 – 1650; b) A. A. Herzing, C. J. Kiely, A. F. Carley, P. Landon, G. J. Hutchings, *Science* **2008**, *321*, 1331 – 1335.
[16] P. Meriaudeau, J. Vedrine, *J. Chem. Soc. Faraday Trans.* **1976**, *72*, 472 – 480.
[17] H. Liu, A. Kozlov, A. Kozlova, T. Shido, K. Asakura, Y. Iwasawa, *J. Catal.* **1999**, *185*, 252 – 264.
[18] M. Kahlich, H. Gasteiger, R. Behm, *J. Catal.* **1997**, *171*, 93 – 105.

Received: November 17, 2015
Published online: January 19, 2016

